

Furthermore, this arrangement allows simultaneously the parallel organization of the rodlike molecules and the segregation of polar and lipophilic units into different regions.

A novel case of mesophase induction by self assembly directed by molecular recognition has been described. It is the first example of mesophase stabilization and induction by interaction of alkali metal cations with a low molecular weight calamitic crown compounds. It is especially remarkable, that this *rod-shaped* molecule can organize as a *columnar* mesophase. In all previously reported cases of mesophase induction by complex formation of crown ethers with alkali metal ions, columnar mesophases were only obtained with tapered-shaped molecules, that is, compounds that have a "pre-disc" shape.

Received: October 9, 1996 [Z96361E]
German version: *Angew. Chem.* 1997, 109, 1160–1163

Keywords: crown compounds · liquid crystals · mesophases · molecular recognition · supramolecular chemistry

- [1] C. J. Pedersen, *J. Am. Chem. Soc.* 1967, 89, 7017; C. J. Pedersen, H. K. Frensdorf, *Angew. Chem.* 1972, 84, 16; *Angew. Chem. Int. Ed. Engl.* 1972, 11, 16; see also C. J. Pedersen, *ibid.* 1988, 100, 1053 and 1988, 29, 1021.
- [2] G. X. He, F. Wada, K. Kikukawa, T. Matsuda, *J. Chem. Soc. Chem. Commun.* 1987, 1294; G. X. He, F. Wada, K. Kikukawa, S. Shinkai, T. Matsuda, *J. Org. Chem.* 1990, 55, 541, 548.
- [3] X. Minggui, Q. Jun, H. Feng, *Mol. Cryst. Liq. Cryst.* 1991, 209, 309.
- [4] V. Percec, V. Rodenhouse, *Macromolecules* 1989, 22, 2043.
- [5] V. Percec, G. Johansson, R. Rodenhouse, *Macromolecules* 1992, 25, 2563.
- [6] J. M. Lehn, J. Malthete, A. Levelut, *J. Chem. Soc. Chem. Commun.* 1985, 1794.
- [7] A. Liebmman, C. Mertesdorf, T. Plesniviy, H. Ringsdorf, J. H. Wendorff, *Angew. Chem.* 1991, 103, 1358; *Angew. Chem. Int. Ed. Engl.* 1991, 30, 1375.
- [8] G. Lattermann, S. Schmidt, R. Kleppinger, J. H. Wendorff, *Adv. Mater.* 1992, 4, 30.
- [9] V. Percec, G. Johansson, J. Heck, G. Ungar, S. V. Batty, *J. Chem. Soc. Perkin Trans. 1* 1993, 1411; V. Percec, J. Heck, G. Johansson, D. Tomazos, G. Ungar, *Macromol. Symp.* 1994, 77, 237, and references therein.
- [10] Columnar mesophases were induced by complexation of rod-coil molecules containing terminal poly(ethylene oxide) chains with LiOTf: M. Lee, N.-K. Oh, *Mol. Cryst. Liq. Cryst.* 1996, 280, 283.
- [11] F. Hildebrandt, J. A. Schröter, C. Tschierske, R. Festag, R. Kleppinger, J. H. Wendorff, *Angew. Chem.* 1995, 107, 1780; *Angew. Chem. Int. Ed. Engl.* 1995, 34, 1631.
- [12] F. Hildebrandt, J. A. Schröter, C. Tschierske, R. Festag, M. Wittenberg, J. H. Wendorff, *Adv. Mater.* 1997, 9, 564–566.
- [13] Obtained by esterification of 4,4'-didecyloxy-*p*-terphenyl-2'-carboxylic acid [11] with hydroxymethyl[18]crown-6 (Aldrich) in the presence of *N*-cyclohexyl-*N'*-[2-(4-methylmorpholino)ethyl]carbodiimide (Aldrich) and catalytic amounts of 4-dimethylaminopyridine. All analytical data agree with the proposed structure for 1: $^1\text{H NMR}$ (500 MHz, CDCl_3 , 25 °C, TMS): δ = 0.87 (t, J = 6.7 Hz, 6H, CH_3), 1.21–1.51 (m, 28H, CH_2), 1.74–1.83 (m, 4H, $\text{ArOCH}_2\text{CH}_2$), 3.30 (dd, J = 14.8, 4.2 Hz, 1H, $\text{OCHCH}_2\text{H}_\text{a}$), 3.37 (dd, J = 16.8, 6.05 Hz, 1H, $\text{OCHCH}_2\text{H}_\text{b}$), 3.54–3.67 (m, 21H, $\text{OCH}_2\text{CH}_2\text{O}$, CH), 3.95 (t, J = 6.3 Hz, 2H, ArOCH_2), 3.99 (t, J = 6.5 Hz, 2H, ArOCH_2), 4.11 (dd, J = 15.1, 5.5 Hz, 1H, $\text{CO}_2\text{CH}_2\text{H}_\text{a}$), 4.20 (dd, J = 16.6, 5.05 Hz, 1H, $\text{CO}_2\text{CH}_2\text{H}_\text{b}$), 6.90 (dd, J = 8.7, 2.0 Hz, 2H, arom. H), 6.96 (dd, J = 8.7, 2.0 Hz, 2H, arom. H), 7.25 (dd, J = 8.7, 2.0 Hz, 2H, arom. H), 7.36 (d, J = 8.0 Hz, 1H, arom. H), 7.54 (dd, J = 8.7, 2.0 Hz, 2H, arom. H), 7.66 (dd, J = 8.1, 2.0 Hz, 1H, arom. H), 7.93 (d, J = 2.0 Hz, 1H, arom. H); MS (70 eV): m/z (%) = 862(100, [M⁺]), 586(13), 569(8), 442(5), 429(13).
- [14] These penetration experiments cannot give precise data concerning the water concentration. Related open-chain compounds can take up to 10 molequiv of water: J. A. Schröter, C. Tschierske, M. Wittenberg, J. H. Wendorff, unpublished results.
- [15] R. M. Izatt, J. S. Brandshaw, S. A. Nielsen, J. D. Lamb, J. J. Christensen, D. Sen, *Chem. Rev.* 1985, 85, 271; R. M. Izatt, R. E. Terry, B. L. Maymore, L. D. Hansen, N. K. Dalley, A. G. Avondet, J. J. Christensen, *J. Am. Chem. Soc.* 1976, 98, 7620.
- [16] The dependence of the clearing temperature on the anions can be caused by several influences. The equilibrium constants of the crown/M⁺/X⁻/water systems should depend on X⁻. However, the differences are small (lgK(KCl) = 1.97; lgK(KBr) = 1.98; lgK(KI) = 1.94; Y. Liu, J. Hu, *Wuli Huaxue Xuebao* 1987, 3, 11; R. M. Izatt, K. Pawlak, J. S. Brandshaw, R. L. Bruening, *Chem. Rev.* 1991, 91, 1721) and cannot explain this effect. In addition, the ability to coordinate water decreases, and the lipophilic character of the anions increases in the order Cl⁻ > Br⁻ > I⁻.
- [17] The molecular length is 4.1 nm (CPK models). The layer thickness of the S_x phase of related 4,4'-didecyloxy-*p*-terphenyl derivatives is 3.3 nm [11].
- [18] The layered organization of the terphenyl cores can tolerate rather large polar lateral substituents [1]. Therefore the crossing of the lateral substituents over the terphenyl units in the periphery should be possible. Furthermore, we have recently found columnar mesophases for facial amphiphiles in which lateral diol groups are connected through polyether chains to the rigid cores. However, columnar mesophases can only be found if the lateral hydrophilic group exceeds a certain length [12]. This means that a certain polarity and also a certain length of the lateral groups are important prerequisites for the formation of these ribbon phases.

K₃Sb₇O₉Se₃·3H₂O: The First Crystalline Nanoporous Material with a Photo-Semiconducting Host Structure**

Ulrich Simon,* Ferdi Schüth, Stephan Schunk, Xiqu Wang, and Friedrich Liebau

During the nineties the preparation of nanostructured materials has evolved to an important and promising area for physicists and chemists. The topic of many developments is the designed formation of specific structures of matter, for example the generation of quantum dots, quantum wires, or multiple quantum wells, for integration into microelectronic circuits to miniaturize functional elements.^[1–3]

To generate nanostructures physicists usually adopt preparation methods like electron beam lithography, which create the small from the large structure and are consequently termed "top-down" methods. However, these methods can only generate structures that have a certain size distribution, but not those of uniform size. This is a disadvantage when quantum size properties are investigated, because these properties are very sensitive to structural changes.

In order to cope with this problem, chemistry has evolved an approach that has so far attracted only little attention. Elaborately optimized synthesis and self-assembly techniques have made available nanostructured materials of uniform shape and size, which may be smaller than one nanometer. These approaches start from atomic or molecular precursors and create large from small. Thus, they are termed "bottom-up" methods. Among these materials are many metal and semiconductor clusters^[4] (which in some cases are arranged in superstructures) as well as a large number of meso- to nanoporous solids. The latter consist of a host structure containing cage- or channel-type pores, or both. Guests are occluded in these voids. By far the best known solids of this kind are zeolites and zeolite-type metal oxides,^[2, 5–7] in which the host structure is a porous, three-dimensional, polyhedral framework. Among the metal oxide group are mainly compounds that fulfil the structural demands of semiconductors but are electrical insulators due to their chemical composition.

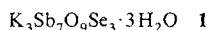
[*] Dr. U. Simon

Institut für Anorganische Chemie der Universität Gesamthochschule Essen
Schützenbahn 70, D-45127 Essen (Germany)
Fax: Int.code + (201)183-2417
e-mail: u.simon@uni-essen.de

Prof. Dr. F. Schüth, Dipl. Chem. S. Schunk
Institut für Anorganische Chemie der Universität Frankfurt (Germany)
Dr. X. Wang, Prof. Dr. F. Liebau
Mineralogisch-petrographisches Institut der Universität Kiel (Germany)

[**] We thank Prof. Dr. M. Czank (Kiel) for the preparation of the electron micrographs, Dr. D. Ackermann (Kiel) for the microprobe analyses as well as Dr. H. Wiggers and J. Jockel (Essen) for their assistance with the impedance measurements. Financial support from the DFG is acknowledged (Li 158/29).

For some time, therefore, efforts have been made to prepare nanoporous semiconducting materials chemically.^[8–10] Such substances are crystallized with templates and typical semiconducting elements such as Sn, Sb, and Se. So far, however, only template-stabilized framework structures that transform into thermodynamically more stable phases and lose their porosity upon removal of the template have been found. Here we report the synthesis of the crystalline, template-free compound **1** with a host structure consisting of one-dimensional tubular chains and discuss its thermal, optical, and electrical properties.



Crystals of **1** are prepared hydrothermally from aqueous KOH and elemental antimony and selenium and grow as dark-red hexagonal prisms to a maximum size of 0.1 mm width and 1 mm length. Under standard conditions ($T = 298 \text{ K}$, $P = 0.1 \text{ MPa}$) they are stable to air, water, methanol, ethanol, and acetic acid. The determination of the structure based on single-crystal X-ray diffraction data^[11] shows that **1** is an ordered $2 \times 2 \times 1$ superstructure of the disordered structure of the natural mineral cetinite $(\text{K}, \text{Na})_{3+x}(\text{Sb}_2\text{O}_3)_3(\text{SbS}_3) \cdot (2.8 - x) \cdot \text{H}_2\text{O}$ ^[12] and a series of synthetic phases that are isotypic with cetinite and that have the general formula $\text{A}_6[\text{Sb}_{12}\text{O}_{18}][\text{SbX}_3]_{12} \cdot (6 - mx - y)\text{H}_2\text{O} \cdot x[\text{B}^{m+}(\text{OH})_m] \cdot y\text{□}$ ($\text{A} = \text{Na}^+, \text{K}^+, \text{Rb}^+$; $\text{X} = \text{S}^{2-}, \text{Se}^{2-}$; and $\text{B} = \text{Na}^+, \text{Sb}^{3+}$).^[13] The square in that formula represents a vacancy in the crystal structure, that is, not all of the H_2O and OH positions have to be occupied (for example after dehydration).

In the hexagonal structure of **1**, pyramidal $[\text{SbO}_3]$ groups are linked to tubular $[\text{Sb}_{12}\text{O}_{18}]$ chains (Figure 1). These tubes are

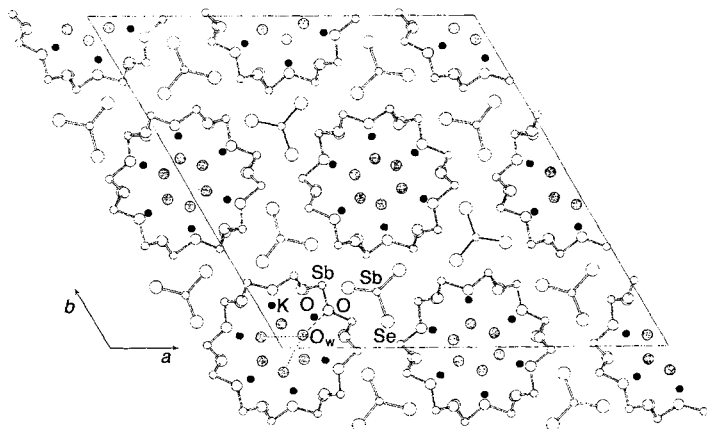


Figure 1. Projection of the hexagonal structure of **1** along the crystallographic c axis ($a = b = 29.260(7)$, $c = 5.6164(7) \text{ \AA}$, $Z = 8$, space group $P6_3$).

then combined to form a three-dimensional nanoporous framework through weaker secondary interactions with interjacent $[\text{SbSe}_3]$ pyramids. The diameter of the tubes is about 7.0 \AA , and they are lined by the K^+ ions. The central part of a tube is occupied by $[(\text{H}_2\text{O})_6]$ octahedra, which are elongated trigonally and linked through shared faces to form a chain of octahedra. The electron micrograph in Figure 2 clearly reveals the nanoporous character of the crystal structure.

By a combination of differential thermal analysis, thermogravimetry, and X-ray diffraction it was shown that the host structure of **1** is stable up to about 570 K in air and up to 710 K in flowing nitrogen at standard pressure (0.1 MPa). At higher temperatures in air, Sb^{III} is oxidized to Sb^{V} and the host structure is destroyed.

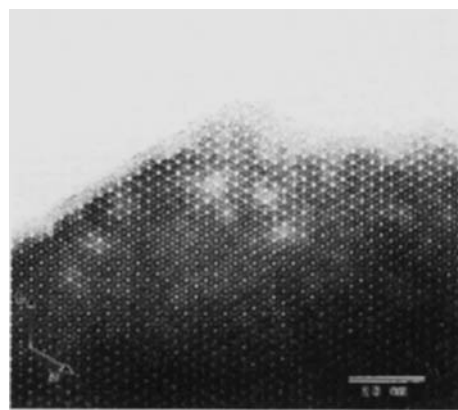


Figure 2. Electron micrograph of **1** showing the nanoporous structure.

Investigations with IR-microspectroscopy using polarized radiation and a high-vacuum sample environment were carried out on single crystals of **1** with a size of $40 \mu\text{m} \times 200 \mu\text{m}$. Figure 3 shows the IR spectra for radiation polarized perpendicular (top) or parallel (bottom) to the hexagonal c axis of the crystals. From these spectra it can be deduced that the water molecules possess a strong preferential orientation in the structure.

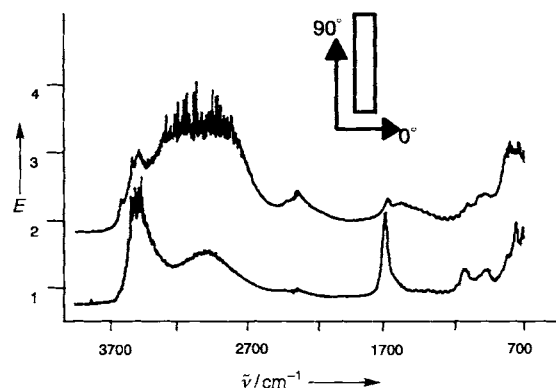


Figure 3. FTIR spectra of a crystal of **1**. The polarization plane is indicated: 0° (top) and 90° (bottom). E = extinction.

A striking characteristic of both spectra is the differences for the two polarization directions in the regions of the OH vibrations (at $3600\text{--}3000 \text{ cm}^{-1}$ and at $1730\text{--}1600 \text{ cm}^{-1}$). The OH vibrations are caused by the water molecules occluded in the channels of **1**. The maxima of the signals occur at around 3500 , 3000 , and 1677 cm^{-1} . This corresponds to the symmetric and antisymmetric stretching modes and the bending mode of free water. The assignment of the high-frequency signal to the symmetric stretching mode is based upon its polarization behavior, which is identical to that of the bending mode. This shows that the two modes belong to the same symmetry.

To verify the assignment of the signals, the water was removed from the channel structure by pumping and heating. In the case of morphologically well-defined crystals, this was achieved at room temperature under high vacuum within a few seconds. In the case of crystal aggregates, which consisted of single crystals intergrown to fiber- or bundlelike units, removal of the water was possible only after grinding and sometimes only after a prolonged treatment at 620 K under vacuum. Because in all cases the IR signals mentioned above vanished under high vacuum, they can unambiguously be identified as belonging to wa-

ter. From the strong polarization of the signal at 1677 cm^{-1} , it can be deduced that the C_2 axis of the water molecules are preferentially aligned parallel to the crystallographic c axis of **1**. From the dichroic ratio a mean deviation of the C_2 axis from the c axis of $20\text{--}30^\circ$ can be calculated.

This is in agreement with the crystallographic result based on the average structure (calculated without consideration of the superstructure reflections), according to which each oxygen atom O_w of the water molecules is attached to an oxygen atom of the tube by a short hydrogen bond of 2.67 \AA (--- in Figure 1). In contrast, distances of 3.12 \AA to two neighboring O_w atoms (··· in Figure 1) indicate the presence of only weak hydrogen bonds. Four such oxygen atoms connected to each other by hydrogen bonds are situated in a plane perpendicular to the c axis.

To determine the optical band gap, single crystals of **1** were studied with a microspectrophotometer (Leica MSV-SP). Figure 4 shows a UV/Vis spectrum that was recorded in transmission mode in the wavelength region between 250 and 800 nm. The solid shows a strong absorption below about 610 nm, which corresponds to the dark-red color of the crystals. This wavelength corresponds to an optical excitation energy of 2.06 eV .

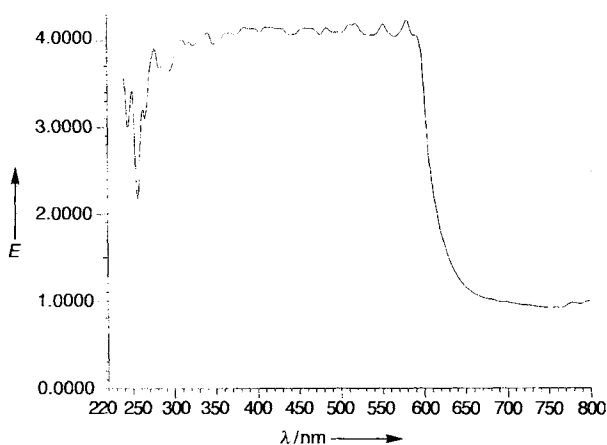


Figure 4. UV-Vis spectrum of **1** measured in transmission mode.

For measurement of the electrical conductivity, single crystals of good optical quality were fixed on a quartz support. Their ends in the c direction were fixed in contact with silver paint. Defects at the crystal surface in the contact region as well as the contacts themselves may influence the results of conductivity measurements.^[14] Therefore, long crystals were selected to make sure that the contribution of the volume to the total conductivity dominates. In addition, the contacts were attached in such a way that they cover the ends of the crystals well enough to minimize the direct incidence of light in this region. Instead of d.c. measurements, impedance measurements were performed in a frequency region from 10 mHz to 10 kHz. With this method interfacial phenomena and contact resistances, for example by an oxide layer, can in most of the cases be separated from the resistance of the volume.^[15]

Figure 5 shows curves of the complex impedance, which are representative of the crystals investigated. Samples were measured in the dark (a) and under illumination with white light (b) at room temperature. The measurements yield compressed semi-circles. From their low-frequency minima, the d.c. resistance R and the specific conductivity σ can be extrapolated. For the example shown here, σ_a (conductivity in the dark) is

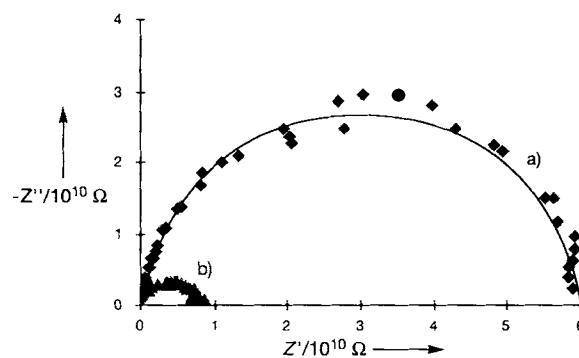


Figure 5. The complex impedance, shown in the complex plane of **1**, in the dark (a) and under illumination (b) at 298 K. The solid line represents an idealized curve fitted through the data by means of a Cole-Cole element.

$2.54 \times 10^{-9}\text{ Scm}^{-1}$ and σ_b (conductivity under illumination with light) is $1.91 \times 10^{-8}\text{ Scm}^{-1}$. As the high-frequency ends of both curves end at the origin of the coordinate system and as only the volume of the crystal was illuminated directly, these results show that **1** is photoconducting. The H_2O guest molecules present in the structure can be excluded as the cause of this conductivity. Accordingly, as far as we know **1** is the first nanoporous semiconductor with a photoconducting host structure.

As at present there is no additional information on the electronic structure of **1** apart from the data presented in this work, no assignment of the optical band gap and no explanation for the basis of photoconductivity can be given. For this purpose, additional investigations, especially on the temperature dependence of the optical absorption and the conductivity, as well as on the mobility of the charge carriers, are in preparation. However, it is clear that with the synthesis and characterization of **1** a step has been made into the direction of potential applications along the lines of the predictions for the class of nanoporous semiconductors.^[2, 5-7] Because of the large interior surface of dehydrated **1**, its use as a highly sensitive and chemoselective sensor appears possible. The results of this work also point to possible optoelectronic and photovoltaic applications.

Experimental Section

Synthesis of **1**: antimony (0.76 g), selenium (0.74 g), KOH (0.80 g), water (2.5 mL), and 2-aminopentane (0.5 mL) were charged into 50 mL teflon bottles, which were sealed and heated to 473 K in a steel autoclave for 4 days. The product was washed with water and methanol, filtered off, and dried in air. As the products always contained minor amounts of other phases, analytical investigations (electron beam microprobe with a CAMEBAX MICROBEAM device from Cameca) and the single crystal X-ray structure determination were carried out on crystals that were selected under the optical microscope.

Received: October 30, 1996 [Z97061E]
German version: *Angew. Chem.* 1997, 109, 1138-1140

Keywords: microporosity · nanostructures · semiconductors · solid-state chemistry

- [1] M. Reed, *Sci. Am.* 1993, (1), 118.
- [2] G. A. Ozin, *Adv. Mater.* 1992, 4, 612.
- [3] U. Simon, G. Schön, G. Schmid, *Angew. Chem.* 1993, 105, 264; *Angew. Chem. Int. Ed. Engl.* 1993, 32, 250; G. Schön, U. Simon, *Colloid Polym. Sci.* 1995, 273, 101; *ibid.* 1995, 273, 202.
- [4] H. Weller, *Angew. Chem.* 1996, 108, 1159; *Angew. Chem. Int. Ed. Engl.* 1996, 35, 1079; T. Vossmeier, G. Reck, L. Katsikas, E. T. K. Haupt, B. Schulz, H. Weller, *Science* 1995, 267, 1476.
- [5] P. Behrens, *Angew. Chem.* 1996, 108, 561; *Angew. Chem. Int. Ed. Engl.* 1996, 35, 515.
- [6] J. V. Smith, *Chem. Rev.* 1988, 88, 149.
- [7] S. L. Suib, *Chem. Rev.* 1993, 93, 803.

- [8] H. Ahari, G. A. Ozin, R. L. Bedard, S. Petrov, D. Young, *Adv. Mater.* **1995**, *7*, 370; P. Enzel, G. S. Henderson, G. A. Ozin, R. L. Bedard, *Adv. Mater.* **1995**, *7*, 64.
 [9] R. L. Bedard, L. D. Vail, S. L. Wilson, E. M. Flanigen, US Pat. 4.880.761, **1989**.
 [10] C. L. Bowes, G. A. Ozin, *Adv. Mater.* **1996**, *8*, 13.
 [11] F. Liebau, X. Wang, *Am. Crystallogr. Ass., Annual Meeting Abstract Book* **1992**, 128.
 [12] C. Sabelli, I. Nakai, S. Katsura, *Am. Mineral.* **1988**, *73*, 398.
 [13] F. Liebau, X. Wang, *Beih. Eur. J. Mineral.* **1995**, *7*, 152; X. Wang, *Z. Kristallogr.* **1995**, *210*, 693.
 [14] R. H. Bube, *Photoconductivity of Solids*, Robert E. Krieger Publishing Company, New York, **1978**.
 [15] J. R. Macdonald, *Impedance Spectroscopy*, Wiley, New York, **1987**.

Highly Efficient Synthesis of Cephalotaxine by Two Palladium-Catalyzed Cyclizations**

Lutz F. Tietze* and Hartmut Schirok

Dedicated to Professor Peter Welzel
on the occasion of his 60th birthday

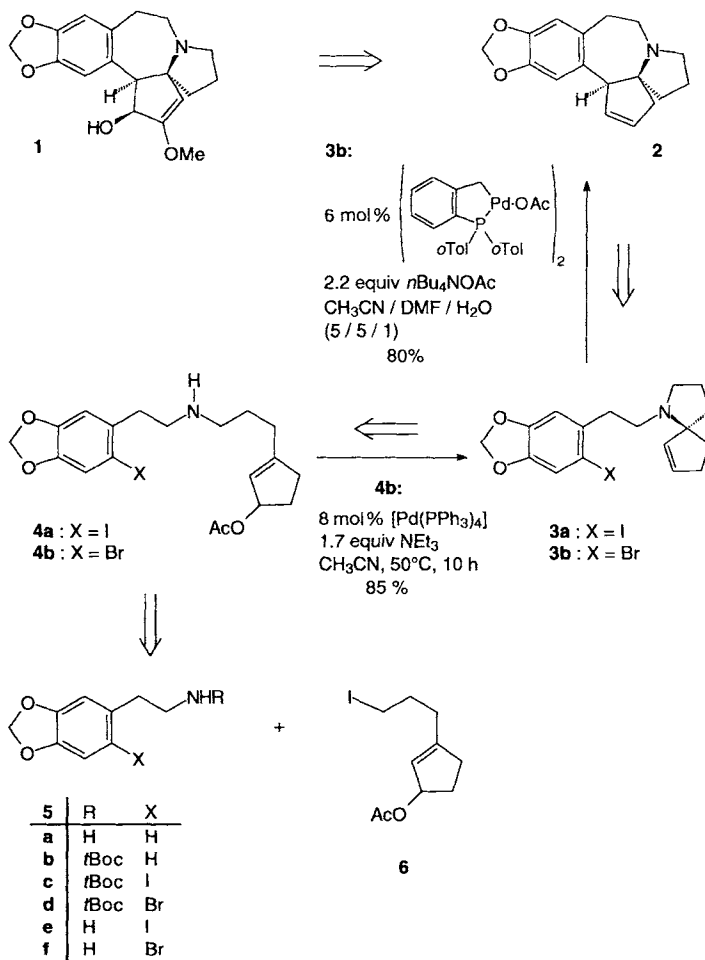
Cephalotaxine **1** is the parent compound of the antileukemic active harringtonines, a group of uniquely structured pentacyclic alkaloids that were isolated from the southeast Asian yew tree of the genus *Cephalotaxus*.^[1] In the harringtonines the free hydroxyl group of **1**, which itself is not biologically active, is esterified by a substituted methyl hydroxymonosuccinate. Although several total syntheses of racemic cephalotaxine have been described,^[2] and even the enantiomerically pure natural product has been synthesized,^[3] new synthetic approaches are especially attractive when they either surpass former methods in efficiency or allow modifications of the structure of the naturally occurring compound.

Both of these requirements are fulfilled by the method reported herein, which is used to construct the racemic intermediate **2**, which, according to Kuehne et al.,^[21] is easily converted in four steps into cephalotaxine **1** in a total yield of 75%. Retrosynthetic analysis of **2** suggests that the cleavage of the seven-membered ring would provide the spirocyclic compound **3a**, which should be available from allyl acetate **4a**. This compound can be readily obtained from **5e** and **6** by alkylation. The intramolecular Pd-catalyzed substitution of an allyl acetate with an amine has already been reported by Godleski et al.,^[4] and the stereoselective construction of benzazepines by intramolecular Heck reaction from appropriate iodoarenes has been carried out with other compounds by our group.^[5] The combination of both Pd-catalyzed reactions should therefore lead to a highly efficient synthesis of cephalotaxine. It had to be clarified first, however, whether the difference in reactivity between the allyl acetates and the iodoarenes is sufficient for a selective reaction process.

For the synthesis of **5e**,^[6] amine **5a**,^[7] readily available from piperonal, was protected with di-*tert*-butyldicarbonate to form **5b** and subsequently halogenated with iodine and silver trifluoroacetate^[8] to yield **5c**. Subsequent cleavage of the *tert*-butoxycarbonyl (*t*Boc) protecting group with trifluoroacetic acid provided the known amine **5e** in 91% yield. Initially, the iodina-

[*] Prof. Dr. L. F. Tietze, Dipl.-Chem. H. Schirok
Institut für Organische Chemie der Universität
Tammannstrasse 2, D-37077 Göttingen (Germany)
Fax: Int. code +(551)39-9476

[**] This research was supported by the Deutsche Forschungsgemeinschaft (Sonderforschungsbereich 416) and the Fonds der Chemischen Industrie. We thank the Degussa AG for their generous donation of precious metals.



tion of **5b** proved difficult. By other methods, such as the reaction with iodine and iodic acid as reported by Königstein,^[9] **5c** was obtained only in very low yields. This results from the fact that the electron density of methylenedioxyarenes such as **5b** is lower than that of 1,2-dimethoxybenzene, because the steric arrangement of the methylenedioxy group restricts the overlapping of the oxygen atoms' orbitals containing nonbonding electron pairs with the π -orbitals of the arene.^[10]

Alkylation of **5e** with iodide **6** (Table 1), readily available from 3-ethoxycyclopentenone in four steps, provides the secondary amine **4a**, the starting material for the double cycliza-

Table 1. ¹H NMR spectroscopic data of **2**, **3b**, **4b**, and **6**.

2: ¹H NMR (200 MHz, CDCl₃): δ = 1.66–1.87 (m, 2H), 1.91–2.07 (m, 3H), 2.34 (dd, J = 14.2, 6.1 Hz, 1H), 2.43 (ddd, J = 9.3, 9.3, 6.8 Hz, 1H), 2.58 (dd, J = 11.7, 7.3 Hz, 1H), 2.76 (ddd, J = 17.8, 4.9, 2.4 Hz, 1H), 2.96 (ddd, J = 12.7, 11.7, 6.1 Hz, 1H), 3.11 (ddd, J = 9.3, 7.6, 4.9 Hz, 1H), 3.20 (ddd, J = 14.2, 12.7, 7.3 Hz, 1H), 3.88 (br. s, 1H), 5.52 (ddd, J = 5.9, 4.4, 2.2 Hz, 1H), 5.79 (ddd, J = 5.9, 5.1, 2.4 Hz, 1H), 5.88 (d, J = 1.5 Hz, 1H), 5.89 (d, J = 1.5 Hz, 1H), 6.59 (s, 1H), 6.65 (s, 1H)

3b: ¹H NMR (200 MHz, CDCl₃): δ = 1.61 (tt, J = 6.8, 6.8 Hz, 1H), 1.74–1.98 (m, 5H), 2.30 (td, J = 7.1, 2.2, 2.1 Hz, 2H), 2.38–2.56 (m, 2H), 2.69–2.85 (m, 3H), 2.88–3.02 (m, 1H), 5.56 (dt, J = 5.6, 2.1 Hz, 1H), 5.80 (dt, J = 5.6, 2.2 Hz, 1H), 5.93 (s, 2H), 6.71 (s, 1H), 6.96 (s, 1H)

4b: ¹H NMR (500 MHz, CDCl₃): δ = 1.7 (br. s, 1H), 1.71 (tt, J = 7.3, 7.3 Hz, 2H), 1.83 (dddd, J = 14.2, 8.7, 3.9, 3.2 Hz, 1H), 2.02 (s, 3H), 2.12–2.25 (m, 3H), 2.32 (dddd, J = 13.9, 8.8, 7.6, 5.1 Hz, 1H), 2.41–2.49 (m, 1H), 2.68 (t, J = 7.2 Hz, 2H), 2.82–2.89 (m, 4H), 5.47 (m, 1H), 6.62–6.66 (m, 1H), 5.95 (s, 2H), 6.74 (s, 1H), 6.99 (s, 1H)

6: ¹H NMR (200 MHz, C₆D₆): δ = 1.35 (tt, J = 7.1, 7.1 Hz, 2H), 1.59 (s, 3H), 1.47–1.71 (m, 4H), 2.49 (t, J = 6.8 Hz, 2H), 5.32 (m, 1H), 5.53–5.64 (m, 1H)